HHS Public Access

Author manuscript

*J Bone Miner Res*. Author manuscript; available in PMC 2015 July 10.

Published in final edited form as:

*J Bone Miner Res*. 2013 November ; 28(11): 2357–2367. doi:10.1002/jbmr.1966.

# In Vivo Tibial Compression Decreases Osteolysis and Tumor Formation in a Human Metastatic Breast Cancer Model

**Maureen E Lynch**[1], **Daniel Brooks**[1], **Sunish Mohanan**[2], **Min Joon Lee**[1], **Praveen Polamraju**[1], **Kelsey Dent**[1], **Lawrence J Bonassar**[1,2], **Marjolein C H van der Meulen**[1,3,4], and **Claudia Fischbach**[1,5]

[1]Biomedical Engineering, Cornell University, Ithaca, NY, USA

[2]Biomedical Sciences, School of Veterinary Medicine, Cornell University, Ithaca, NY, USA

[3]Mechanical and Aerospace Engineering, Cornell University, Ithaca, NY, USA

[4]Research Division, Hospital for Special Surgery, New York, NY, USA

[5]Kavli Institute at Cornell for Nanoscale Science, Cornell University, Ithaca, NY, USA

## Abstract

Bone metastasis, the leading cause of breast cancer-related deaths, is characterized by bone degradation due to increased osteoclastic activity. In contrast, mechanical stimulation in healthy individuals upregulates osteoblastic activity, leading to new bone formation. However, the effect of mechanical loading on the development and progression of metastatic breast cancer in bone remains unclear. Here, we developed a new in vivo model to investigate the role of skeletal mechanical stimuli on the development and osteolytic capability of secondary breast tumors. Specifically, we applied compressive loading to the tibia following intratibial injection of metastatic breast cancer cells (MDA-MB231) into the proximal compartment of female immunocompromised (SCID) mice. In the absence of loading, tibiae developed histologically-detectable tumors with associated osteolysis and excessive degradation of the proximal bone tissue. In contrast, mechanical loading dramatically reduced osteolysis and tumor formation and increased tibial cancellous mass due to trabecular thickening. These loading effects were similar to the baseline response we observed in non-injected SCID mice. In vitro mechanical loading of MDA-MB231 in a pathologically relevant 3D culture model suggested that the observed effects were not due to loading-induced tumor cell death, but rather mediated via decreased expression of genes interfering with bone homeostasis. Collectively, our results suggest that mechanical loading inhibits the growth and osteolytic capability of secondary breast tumors after their homing to the bone, which may inform future treatment of breast cancer patients with advanced disease.

### Keywords

METASTASIS; OSTEOLYSIS; BREAST CANCER; MECHANICAL LOADING

Address correspondence to: Claudia Fischbach, PhD, Cornell University, 157 Weill Hall, Ithaca, NY 14853, USA. Cf99@cornell.edu.

Additional Supporting Information may be found in the online version of this article

**Disclosures**

All authors state that they have no conflicts of interest.

## Introduction

Bone metastasis is the leading cause of breast cancer–related deaths among women worldwide[1] and increases patient morbidity and mortality by promoting nerve compression, pain, bone fragility and fracture, and hypercalcemia.[2–4] In healthy individuals, homeostatic bone remodeling involves bone resorption by osteoclasts and replacement by bone-forming osteoblasts. However, in the presence of a tumor, the relative activities of these two cell types are perturbed, and overall bone mass is reduced because tumor cells enhance the concentration of pro-osteoclastic factors within bone.[4,5] The resulting increase in osteoclastogenesis stimulates net resorption and release of pro-tumorigenic growth factors from the bone extracellular matrix, thereby activating the "vicious cycle" of osteolytic bone metastasis.[6]

Because metastatic breast cancer frequently localizes to regions of cancellous bone that are load-bearing (eg, hip, spine) and therefore more susceptible to fracture, bed rest is sometimes prescribed for patients with high risk for fracture. Yet the skeleton is sensitive to its mechanical environment, and lack of physical stimulation, eg, due to bed rest, promotes bone loss.[7,8] In contrast, mechanical loading can increase bone mass due to its ability to upregulate osteoblast activity[9,10] and may prove beneficial for diseases associated with excessive osteolytic bone remodeling as has been shown for osteoporosis.[11,12] In fact, physical exercise shows promise as an adjuvant therapy for breast cancer patients.[13,14] However, the role of mechanical stimulation in breast cancer–associated osteolytic bone remodeling is largely unknown. Here, we propose that mechanical stimulation represents an important microenvironmental parameter regulating the growth and osteolytic capability of secondary breast tumors in bone.[15]

In vivo models of controlled loading have previously been established to determine the effect of specific loading parameters on bone formation. For example, increased strain rate enhances the skeletal response to loading,[16] a result that has been incorporated into exercise therapy regimes for postmenopausal women.[17] Furthermore, tibial compression elevates cancellous bone mass in hormone-deficient, osteoporotic mice and prevents bone loss in aged mice.[18,19] Here, our goal was to build on these studies and develop an in vivo loading model of secondary metastatic tumor growth in bone to determine whether mechanical stimulation of bone plays a role in metastasis-driven osteolysis and tumor formation. To accomplish this goal, we injected human breast cancer cells into the proximal tibia of immunocompromised mice prior to applying tibial compression. Because the loading response of these mice is unknown, we first determined the relationship between applied compression and bone tissue deformation through strain-gauging of the cortex. Subsequently, we investigated the hypothesis that mechanical loading increases cancellous bone mass and inhibits resorption, thereby inhibiting tumor establishment and growth. To investigate our hypothesis, we assessed overall bone mass and architecture and tissue composition as a function of loading via micro–computed tomographic and histological analysis, respectively. To evaluate specific molecular mediators underlying loading-induced changes in tumor cell behavior under well-defined conditions, we additionally applied

compressive mechanical loading to a 3D mineral-containing culture model seeded with human metastatic breast cancer cells.

## Subjects and Methods

### Animals

Female severe-combined immunodeficient (SCID; Jackson Laboratory, Bar Harbor, ME, USA) mice were housed 3 to 5 animals per cage with *ad libitum* access to food and water. Body masses were recorded daily and used to monitor the health of the mice over the course the experiment. All experimental procedures using animals were performed in accordance with Cornell University's Institutional Animal Care and Use guidelines.

### In vivo load-strain calibration

To establish the relationship between applied tibial compression and bone tissue deformation for SCID mice, the left tibiae of 5 mice were strain-gauged and loaded using methods previously established.[20] This relationship was used to determine the peak applied force that engendered +600 $\mu\varepsilon$ at the medial midshaft of the tibia, as representative of physiological high-strain conditions of a mouse during a 30 cm jump.[21] In brief, a single-element strain-gauge (EA-06-015LA-120; Micro-measurements, Raleigh, NC, USA) was attached to the medial surface of the tibial midshaft aligned with the bone's long axis (Fig. 1C). While mice were anesthetized (2% isoflurane, 1.0 L/min; Patterson Veterinary, Devens, MA, USA), a range of dynamic compressive loads (peak loads ranging from −3 to −15 N) was applied, and strain measurements recorded simultaneously (Labview v8.2; National Instruments, Austin, TX, USA) (Fig. 1A). The slopes of the strain-load regressions were −0.0068 N/$\mu\varepsilon$ (95% CI, −0.0078 to −0.0058). A peak compressive load of 4.1 N induced +600 $\mu\varepsilon$ in SCID mice and was applied in all further experiments (Fig. 1B).

### Tumor cells and tumor inoculation

MDA-MB231 human breast cancer cells (MDAs; ATCC, Manassas, VA, USA) were maintained in complete DMEM (DMEM [Invitrogen, Carlsbad, CA, USA] supplemented with 10% fetal bovine serum [Tissue Culture Biologicals, Long Beach, CA, USA] and 1% penicillin/streptomycin [Invitrogen]) under standard cell culture conditions (37°C, 5% $CO_2$).

At 7 weeks of age, 46 mice were randomized into tumor ($n$ = 24) and control ($n$ = 22) groups. MDAs were injected into the left tibiae of the tumor group as described.[22–24] PBS alone was sham-injected into tibiae of the control group. Briefly, mice were anesthetized as previously described and tibiae were surgically exposed. With the knee in the flexed position, the cell suspension ($5 \times 10^5$ cells suspended in 20 μL sterile PBS) or PBS (20 μL) was injected through the tibial plateau with a 27-gauge needle into the marrow space of the proximal compartment.

### In vivo tibial compression

One day following injection, mice were further randomized into loaded and nonloaded groups (tumor: $n$ = 12/group, control: $n$ = 10–12/group). Typically, loading studies use the contralateral limb as an internal, nonloaded control.[25] However, because tumor-derived

circulating factors can have systemic effects, separate animals were used to compare loaded and nonloaded tumor-bearing tibiae. For loading, the left limbs of mice were subjected to dynamic compressive loading for 2 or 6 weeks using an established protocol (1200 cycles at 4 Hz, 5 days/week)[26]; nonloaded control mice only underwent anesthesia. During all loading sessions, mice were maintained under general anesthesia as previously described. Normal cage activity was allowed between loading sessions. Appropriate localization of tumor cells to the intratibial cavity was confirmed via in vivo bioluminescent imaging following injection of luciferase-expressing MDAs in a separate group of animals (Supplementary Fig. S1).

To characterize the baseline adaptive response of SCID mice in the absence of intratibial sham injections, 10 mice underwent tibial compression for 2 or 6 weeks ($n$ = 5/group). For these studies, the right limb served as the nonloaded, internal control.

At experimental endpoints, mice were euthanized by $CO_2$ inhalation. Tibiae were dissected free of soft tissue, fixed in 10% neutral buffered formalin for 48 hours, and then stored in 70% ethanol.

## Micro–computed tomography

Cancellous bone mass and architecture and total tibial length were assessed using quantitative micro–computed tomography (μCT) (μCT35; Scanco Medical AG, Brüttisellen, Switzerland; 55 kVp, 145 mA, 600-ms integration time, no frame averaging). A 0.5-mm aluminum filter reduced the effects of beam hardening. Proximal and whole tibiae were scanned at 15-μm and 20-μm isotropic resolution, respectively. Cancellous volumes of interest (VOIs) were defined in all left tibia. The purely cancellous VOI began approximately 0.5 mm distal to the growth plate, excluding the primary spongiosa and cortical shell, and extended 10% of the total tibial length. Cancellous mineralized tissue was segmented from water and soft tissue using a global threshold determined for each group (247–280 mg hydroxyapatite [HA]/mL). Cancellous outcomes included bone volume fraction (BV/TV), and trabecular thickness and separation (Tb.Th and Tb.Sp, μm). Whole bones were aligned similarly along the longitudinal axis, and total length was measured from the minimum point of the growth plate to the most distal end.

## Histology

Tibiae were decalcified in ethylenediaminetetraacetic acid (10% EDTA, pH 7.4) and embedded in paraffin. Serial, longitudinal, 7-μm thick sections were cut from each sample. Sections were deparaffinized in xylene, rehydrated in an ethanol gradient, and stained with hematoxylin and eosin (H&E) and for the osteoclast marker tartrate-resistant acid phosphatase (TRAP) using standard procedures. Images of complete histological sections were captured using an Aperio Scanscope (Aperio, Vista, CA, USA). Evaluation of tumor formation, inflammatory responses, and osteoblast and osteoclast activation were assessed on consecutive H&E-stained histological longitudinal cross-sections by a board-certified pathologist (SM).

### Characterization of loading effects in a 3D culture model

The direct effects of mechanical loading on tumor cells were determined by applying compressive forces to a 3D tumor model based on mineral-containing porous scaffolds that recapitulate bone materials properties.[27] Scaffolds were prepared from poly(lactide-co-glycolide) (PLG) and HA using established methods.[27,28] Briefly, 8 mg of PLG microspheres, 8 mg of HA particles (Sigma-Aldrich, St. Louis, MO, USA; average diameter of 200 nm), and 152 mg of NaCl particles sized 250 to 400 μm (J.T. Baker, Center Valley, PA, USA) were pressure-molded (Carver Press, Wabash, IN, USA) into disks (1 mm thick, 8 mm in diameter). These disks were subsequently subjected to a gas-foaming/particulate leaching technique that results in surface exposure of the incorporated mineral.[29] Mechanical characterization of the scaffolds ($n = 4$) was conducted for both quasi-static and dynamic loading conditions.

Scaffolds were sterilized with 70% ethanol, washed four times with sterile PBS, and seeded with 1.5 million MDAs per scaffold as previously described.[27] Cell-seeded scaffolds were maintained on an orbital shaker at 37°C and 5% $CO_2$ for 3 days prior to loading to encourage 3D tissue formation. For loading experiments, these tumor constructs were randomized into loaded and nonloaded groups ($n = 3$–4/group). The loading platen of an established loading bioreactor was adapted for applying mechanical forces to scaffolds in a 24-well plate (Fig. 7B).[30] Scaffolds underwent compressive loading for 1 hour per day for 3 days. During loading, a 5% amplitude sinusoidal strain at 1 Hz was superimposed on a 5% static strain offset. These loading parameters were chosen because they have been previously reported to stimulate osteoblasts.[31,32] Scaffolds were maintained on the orbital shaker in between loading sessions and 24 hours after the final session, they were harvested for gene expression, DNA analysis, live/dead staining, and histological analysis. Expression of genes commonly associated with bone metastasis (OPN, MMP1, and CXCR4)[33] and osteolysis (IL-8, RANK, Runx2, DKK1)[5,34–38] was determined using quantitative RT-PCR (qPCR) and the comparative delta-cycle threshold ($\Delta C_T$) method.[39] Briefly, mRNA was isolated from scaffolds using the TRIzol extraction method[40] in RNase-free conditions. qPCR was performed using SYBR for the genes of interest and normalized to the expression of β-actin (Supplemental Table S1). DNA was isolated with Caron's buffer and quantified using a Quantifluor fluorescent dye (Promega, Madison, WI, USA). Live cells were stained with calcein and dead cells were stained with propidium iodide.

### Statistical analysis

The effects of in vivo loading, tumor, and experimental duration were determined using a second-degree linear mixed-model (JMP v9.0; SAS Institute, Cary, NC, USA). For loading effects, the between-subject factor was limb, loaded or nonloaded control; for tumor effects, tumor or PBS injection; and for duration, 2 or 6 weeks. In the baseline experiment, the effects of loading and duration were determined using a full factorial linear mixed-model, in which for loading effects, the within-subject factor was limb, loaded or control (left or right tibia), and the between-subject factor was duration, 2 or 6 weeks. To determine the effects of injection, the adaptive response of control mice was compared to sham-injected mice using a full factorial linear mixed-model, in which for loading effects, the within-subject factor was limb, loaded or control (left or right tibia), and the between-subject factor was injection

status, sham-injected or intact bone. For in vitro loading studies, experiments were performed in duplicate, and the results reflect pooled data. The effect of loading was determined using two-tailed *t* tests. For all statistical analyses, main effects are reported and data pooled if no significant interaction was present. Otherwise, group means were compared using a post hoc Tukey-Kramer test with a Bonferroni correction. Statistical significance was set at $\alpha \leq 0.05$. All values are represented as mean ± SD.

## Results

### Tumor-mediated bone degradation as a function of mechanical loading

To analyze the integrated effects of mechanical loading and human metastatic breast cancer on bone remodeling, we injected MDAs into the tibiae of immunocompromised mice and subsequently applied tibial compression. Macroscopic inspection of explanted tibiae followed by global analysis via μCT and histology revealed that all of the proximal tibiae of nonloaded, tumor-injected mice contained histologically detectable tumors (100% of animals, Figs. 2C, D, 3B) and nearly all were completely degraded (71% of animals, Figs. 2A, B, 3B) after 6 weeks. In contrast, tibial compression markedly reduced tumor development and bone degradation, resulting in tibial features similar to sham-injected control mice (Fig. 2A–D). Further evaluation of the nonloaded tumor group indicated that 20% of mice developed histologically detectable tumors within 2 weeks, whereas no obvious evidence of bone degradation was observed by μCT in these animals (Figs. 2A, B, 3A–C).

To further analyze the kinetics of tumor-mediated bone degradation as a function of loading, the mass and architecture of the cancellous bone in the proximal compartment were assessed via μCT analysis after 2 and 6 weeks. After 2 weeks, both BV/TV and Tb.Th in control and tumor-injected tibiae were similar in the nonloaded groups, indicating no obvious bone degradation after this time period despite the presence of tumor cells (Figs. 4A, B). In contrast, a marked difference was noted after 6 weeks: as mentioned above, 71% of tumor-bearing tibiae were degraded, causing the exclusion of this group from more detailed μCT analysis (Figs. 3A, 4). Interestingly, 2 weeks of loading significantly enhanced BV/TV (160%) and Tb.Th (97%) in tumor-bearing tibiae relative to the respective nonloaded tibiae; in the sham-injected control group a similar, but not statistically significant, trend was noted. After 6 weeks, these differences were even more pronounced: tibial loading enhanced BV/TV in both the absence of and in the presence of tumor cells. Specifically, the previously noted substantial bone degradation present in tumor-injected animals was prevented by loading, and BV/TV and Tb.Th values for these tibiae were statistically similar to loaded control tibiae; ie, even greater than for tibiae of nonloaded control animals (Fig. 4A, B). Tb.Sp was not altered under any experimental condition (Fig. 4C). Tibial length did not differ among groups at any time point (16.2 ± 0.3 mm, pooled average). Body masses were equal among groups at the start of the experiment (17.9 ± 1.7 g, pooled average), and increased similarly over the 6-week course of the experiment for all experimental conditions (Control: 21.1 ± 1.2 g [nonloaded]; 19.7 ± 1.2 g [loaded]; Tumor: 19.6 ± 1.4 g [nonloaded]; 20.0 ± 1.9 g [loaded]).

To characterize the combined effects of loading and intratibial tumor growth on bone remodeling at the cellular level, we analyzed histological cross-sections from each experimental condition. Evaluation of H&E-stained sections revealed that tumor formation remained localized to the injection site in 20% of nonloaded mice after 2 weeks, whereas tumor formation and invasion were extensive after 6 weeks and resulted in widespread degradation of the tibial proximal metaphysis (Figs. 3B, 5A, B). An appreciably different pattern was observed in tibiae of loaded animals. No evidence of tumor formation was detected in H&E-stained tibial sections prepared from animals undergoing both tumor injection and loading after 2 weeks, and only 29% of loaded animals versus 100% of nonloaded animals developed tumors after 6 weeks (Figs. 3B, 5A, B). Activated osteoblasts on skeletal surfaces were noted in loaded tibiae after 2 and 6 weeks, whereas mature, multinucleated osteoclasts were associated with bone surfaces in the nonloaded 6 week group next to developed tumors (Fig. 5B, C).

### Baseline adaptive response of immunocompromised SCID mice

As the baseline adaptive response to loading of SCID mice has not previously been characterized and to ensure that the above-described effects of loading were not artificially introduced by the intratibial injections, we tested the effect of tibial compression in intact; ie, non-injected animals. Six weeks of loading increased cancellous bone mass in SCID mice, primarily through trabecular thickening (Fig. 6A). BV/TV was 130% greater in loaded tibiae relative to nonloaded tibiae after 6 weeks (Fig. 6B). After 2 weeks, Tb.Th was 36% greater in loaded tibiae relative to nonloaded tibiae, and increased further with continued loading (+74%, after 6 weeks). Although Tb.Sp was similar between sham-injected and intact tibiae for the individual time points, overall, Tb.Sp decreased with loading (−35%, pooled loaded versus nonloaded groups). Tibial length did not differ among groups at any time point (16.2 ± 0.2 mm, pooled average). Furthermore, initial body masses and weight gain over the course of the experiment were similar between groups (initial weight: 19.6 ± 1.2 g, pooled average; weight after 6 weeks: 19.9 ± 0.6 g).

Additional comparison of SCID mice with and without sham injection suggested that the injection procedure modulated the initial, but not the prolonged tibial response to loading. Although loading had no effect on cancellous mass of intact tibiae after 2 weeks, BV/TV of sham-injected tibiae increased after 2 weeks of loading (Supplementary Fig. S2). Additionally, the sham-injected group had thicker trabeculae (Tb.Th: +24%, pooled PBS versus pooled Intact), but Tb.Sp was maintained. By 6 weeks, however, the adaptive response normalized and no difference was observed between the sham-injected and intact groups for any μCT measure. Furthermore, indications of an acute inflammatory response were present at the injection site (eg, mature neutrophil invasion) after 2 weeks, but not after 6 weeks (data not shown).

### Tumor cell response to mechanical loading

To probe potential molecular mediators underlying our in vivo results, we modified an existing in vitro loading model by applying mechanical compression to a mineral-containing 3D tumor construct (Fig. 7B). To ensure that applied mechanical loads were within the linear elastic range of the scaffolds, the compressive Young’s modulus and yield strain

under quasi-static uniaxial compression were determined to be 290 ± 20 kPa and 29% ± 9% strain, respectively (Fig. 7A). Additionally, dynamic loading using experimental loading conditions was applied to scaffolds ($n$ = 4) and compressive forces were recorded under constant strain to ensure that strain hardening was not occurring (data not shown). Live and dead staining demonstrated that the vast majority of tumor cells within both loaded and control scaffolds were viable, and similarly, total DNA content was comparable between loaded and control scaffolds after 3 days of loading (Fig. 7C, D). These results suggest that loading has no effect on tumor cell death and growth. Furthermore, mechanical compression did not alter the expression of bone metastasis-specific genes (OPN, MMP1, and CXCR4)[33] nor of genes commonly associated with osteolysis (IL-8, RANK, DKK1).[5,34–38] However, expression of Runx2, which is aberrantly expressed by tumor cells and plays a role in both osteoclast and osteoblast differentiation,[36,38] was reduced 35% with loading (Fig. 7E). Taken together, these results suggest that loading indirectly inhibits tumor growth by modulating the interplay between osteoclasts and osteoblasts.

## Discussion

To investigate the role of loading in bone-associated tumor formation and growth, we developed a new in vivo model that integrates mechanical loading with human metastatic breast cancer, and used this in combination with in vitro loading experiments to understand mechanisms of metastatic tumor growth in bone. In the absence of loading, tumor establishment and bone degradation in our studies was similar to that observed by other groups using intratibial or intrafemoral injection of cancer cells,[23,41,42] whereas loading significantly altered these effects. Specifically, tibial compression dramatically reduced histologically detectable tumor formation and associated osteolytic bone loss. In vitro studies suggested that these effects may not only be related to loading-induced changes in bone cell behavior, but may be partially attributed to mechanically-induced alterations in gene expression in tumor cells.

Possible explanations for the lack of tumor establishment in our studies include that the anabolic skeletal response to loading likely occurred before tumor-mediated osteolysis could take place, thereby preventing activation of the vicious cycle of bone metastasis. Following direct injection, tumors require approximately 4 to 6 weeks to fully establish and develop osteolytic lesions,[23,41,42] whereas bone responds to loading more quickly. Specifically, expression of bone-forming genes and recruitment of osteoblasts occurs within hours,[43,44] and new bone formation is detectable within days.[45] Correspondingly, tibial loading resulted in elevated tissue coverage of activated osteoblasts and marked bone formation as early as 2 weeks, similar to other studies.[21,26,46] Additionally, loading may counteract tumor-mediated osteoclastogenesis that, in turn, may decrease the release of growth factors from the bone matrix, otherwise promoting tumor colonization and expansion.[47] Consistent with this possibility, skeletal tissue coverage by osteoclasts was elevated in tumor-bearing, nonloaded tibiae in our studies. Our observations are supported by other studies demonstrating that loading stimulates osteoblastic over osteoclastic activity.[9,48–50] Finally, mechanical loading can inhibit neovascularization, a hallmark of cancer,[15] which may also contribute to the absence of tumor formation in loaded animals.[51]

Based on our in vitro loading experiments, loading does not directly affect tumor cell growth or death, but rather altered their expression of morphogens that can, in turn, modulate osteoclast and osteoblast functions. Breast cancer cells express factors that promote the formation of osteolytic lesions, such as IL-8,[5] RANK,[34,35] DKK,[38] Runx2,[37,52] and that generally favor their bone-metastatic capability (OPN, MMP1, and CXCR4).[33] Interestingly, mechanical stimulation neither affected expression of the bone-metastatic gene signature nor expression of most pro-osteoclastogenic factors. However, mechanical compression inhibited expression of Runx2, which is known to stimulate osteolysis by upregulating parathyroid hormone-related protein (PTHrP)-induced RANKL secretion by osteoblasts,[53] and its abolishment reduced osteolytic lesions.[37] Furthermore, Runx2 also decreases osteoblast differentiation via altered cancer cell secretion of sclerostin, an inhibitor of Wnt signaling.[36,54] Combined, our in vivo and in vitro results suggest that loading may interfere with osteolysis by upregulating osteoblastic over osteoclastic activity. Future experiments are needed to further characterize the role of Runx2 in the effects of loading on secondary metastatic tumor growth.

The goal of our studies was to determine whether in vivo loading affected human metastatic breast cancer, requiring the use of immunocompromised animals and intratibial injection procedures because human breast cancer cells do not spontaneously metastasize to bone in mice.[55] In comparison to other studies with immunocompetent mice, SCID mice displayed a delayed response to tibial compression after 2 weeks, but after 6 weeks the magnitude of effect was comparable.[18,46] The lack of a fully functional immune system may have contributed to these initial differences as immunity plays a modulatory role in bone remodeling and homeostasis[56,57] and tumorigenesis.[58] Additionally, species-specific differences in paracrine signaling between human and murine cells may have been a regulating factor in our studies. Finally, we observed a mild to moderate acute inflammatory response at the epiphysis and within the marrow associated with the site of injection in the 2 week group, but not in the 6 week group. Therefore, adaptive responses due to the injection procedure may have modulated the initial loading response in our studies. A regional acceleratory phenomena (RAP)[59] induced by the defect created at the injection site may have initiated a localized adaptive response.[60] When combined with mechanical loading, this response may be enhanced because both stimuli promote remodeling. However, this phenomenon was only present initially in our studies; by 6 weeks, both groups exhibited similar adaptive loading responses.

Anabolic mechanical stimulation is generally recommended for treating or preventing pathological bone loss, such as osteoporosis, and may be similarly useful for patients with metastatic bone disease. Clinically, physical activity improves physical functioning and quality of life for patients undergoing or recovering from chemotherapy,[13,61,62] including improved bone measures.[14] However, its ability to prevent or treat bone metastasis and secondary tumor growth is unknown. An unresolved clinical issue in prescribing high-impact exercise, which is the most effective for improving skeletal measures,[17,63] is that patients already exhibit heightened skeletal fragility and pain.[3] However, skeletal fragility is present for nearly all populations with pathological bone loss, for whom exercise has proved beneficial.[11] Additionally, alternate loading modalities, such as low-magnitude

high-frequency vibration, may represent feasible alternatives for patients with advanced metastasis.[64]

The results presented herein show a functional link between mechanical stimulation and breast cancer–induced bone disease and inspire a number of future studies. For example, the fate of the intratibially-injected breast cancer cells following in vivo loading needs to be assessed. These cells could become dormant, undergo apoptosis, or localize to distant sites, although we did not observe any macroscopic signs of tumor development during necropsy of organs typically prone to metastasis (eg, liver, lung). Furthermore, whether loading reduces tumor burden in established secondary tumors and/or plays a role in metastatic homing to bone are unresolved questions that need to be determined in order to translate our findings to clinically relevant scenarios. In the clinic, circulating tumor cells (CTCs) have emerged as a potential biomarker of metastasis[65] that may help identify patient populations suitable for physical therapy and determine the appropriate timing for prescription. Elucidating whether or not loading has a synergistic effect with current adjuvant therapies, such as bisphosphonates, will also inform decisions about the relevance of loading. Finally, examining the sensitivity of cancer cells to loading will reveal the strength of the mechanical signal required for inhibiting cancer-induced bone disease. Such dose response studies will help identify feasible physical therapy strategies for patients at risk for fracture and subject to bone pain.

In conclusion, our results suggest that mechanical loading inhibits secondary growth and osteolytic capability of metastatic tumors by modulating relative osteoblastic and osteoclastic activities, though further work is required to fully understand the molecular mechanisms underpinning these results. Although our studies were designed to study the interplay between mechanical stimulation and secondary breast cancer located in bone, metastatic bone disease from other cancers (eg, prostate, lung) may be similarly examined using this model. In particular, future work exploring the ability of loading to alter a variety of clinically relevant scenarios, such as the prevention and treatment of bone-metastatic tumors, will shed further light on mechanical stimulation as a tumor microenvironmental parameter modulating the clinical outcome of patients with advanced disease.

## Supplementary Material

Refer to Web version on PubMed Central for supplementary material.

## Acknowledgments

This work was supported by NIH/MRRCC 5P30 AR046121-09, 1R01CA173083, R21CA157383, R01-AG028664, NYSTEM, and an Individual Biomedical Research Award by the Hartwell Foundation. We gratefully acknowledge the assistance of Siddharth Pathi with intratibial injections, Lyudmila Lukashova with μCT acquisition analysis, Dr. Stephen Doty with histological staining, Cornell's CARE staff with animal care, and the Musculoskeletal Repair and Regeneration Core Center at the Hospital for Special Surgery for providing access to μCT and histological core facilities.

Authors' roles: Study design: MEL, LB, MvdM, and CF. Data collection: MEL, DB, MJL, and PP. Data analysis: MEL, SM, and KD. Data interpretation: MEL, SM, MvdM, and CF. Drafting manuscript: MEL and CF. Revising manuscript content: MEL, SM, MvdM, and CF. Approving final version of manuscript: all authors. MEL and CF take responsibility for the integrity of the data analysis.

## References


1. Bussard KM, Gay CV, Mastro AM. The bone microenvironment in metastasis; what is special about bone? Cancer Metastasis Rev. 2008; 27:41–55. [PubMed: 18071636]
2. Coleman RE. Metastatic bone disease: clinical features, pathophysiology and treatment strategies. Cancer Treat Rev. 2001; 27:165–76. [PubMed: 11417967]
3. Kozlow W, Guise TA. Breast cancer metastasis to bone: mechanisms of osteolysis and implications for therapy. J Mammary Gland Biol Neoplasia. 2005; 10:169–80. [PubMed: 16025223]
4. Mundy GR. Metastasis to bone: causes, consequences and therapeutic opportunities. Nat Rev Cancer. 2002; 2:584–93. [PubMed: 12154351]
5. Bendre MS, Gaddy-Kurten D, Mon-Foote T, Akel NS, Skinner RA, Nicholas RW, Suva LJ. Expression of interleukin 8 and not parathyroid hormone-related protein by human breast cancer cells correlates with bone metastasis in vivo. Cancer Res. 2002; 62:5571–9. [PubMed: 12359770]
6. Guise TA. The vicious cycle of bone metastases. J Musculoskelet Neuronal Interact. 2002; 2:570–2. [PubMed: 15758398]
7. Donaldson CL, Hulley SB, Vogel JM, Hattner RS, Bayers JH, McMillan DE. Effect of prolonged bed rest on bone mineral. Metabolism. 1970; 19:1071–84. [PubMed: 4321644]
8. Vico L, Collet P, Guignandon A, Lafage-Proust MH, Thomas T, Rehaillia M, Alexandre C. Effects of long-term microgravity exposure on cancellous and cortical weight-bearing bones of cosmonauts. Lancet. 2000 May 6.355:1607–11. [PubMed: 10821365]
9. Hillam RA, Skerry TM. Inhibition of bone resorption and stimulation of formation by mechanical loading of the modeling rat ulna in vivo. J Bone Miner Res. 1995; 10:683–9. [PubMed: 7639102]
10. Chow JW, Wilson AJ, Chambers TJ, Fox SW. Mechanical loading stimulates bone formation by reactivation of bone lining cells in 13-week-old rats. J Bone Miner Res. 1998; 13:1760–7. [PubMed: 9797486]
11. Kerr D, Ackland T, Maslen B, Morton A, Prince R. Resistance training over 2 years increases bone mass in calcium-replete postmenopausal women. J Bone Miner Res. 2001; 16:175–81. [PubMed: 11149482]
12. Kohrt WM, Ehsani AA, Birge SJ Jr. Effects of exercise involving predominantly either joint-reaction or ground-reaction forces on bone mineral density in older women. J Bone Miner Res. 1997; 12:1253–61. [PubMed: 9258756]
13. Milne HM, Wallman KE, Gordon S, Courneya KS. Effects of a combined aerobic and resistance exercise program in breast cancer survivors: a randomized controlled trial. Breast Cancer Res Treat. 2008; 108:279–88. [PubMed: 17530428]
14. Schwartz AL, Winters-Stone K, Gallucci B. Exercise effects on bone mineral density in women with breast cancer receiving adjuvant chemotherapy. Oncol Nurs Forum. 2007; 34:627–33. [PubMed: 17573321]
15. Hanahan D, Weinberg RA. Hallmarks of cancer: the next generation. Cell. 2011; 144:646–74. [PubMed: 21376230]
16. Mosley JR, Lanyon LE. Strain rate as a controlling influence on adaptive modeling in response to dynamic loading of the ulna in growing male rats. Bone. 1998; 23:313–8. [PubMed: 9763142]
17. Stengel SV, Kemmler W, Pintag R, Beeskow C, Weineck J, Lauber D, Kalender WA, Engelke K. Power training is more effective than strength training for maintaining bone mineral density in postmenopausal women. J Appl Physiol. 2005; 99:181–8. [PubMed: 15746294]
18. Fritton JC, Myers ER, Wright TM, van der Meulen MC. Bone mass is preserved and cancellous architecture altered due to cyclic loading of the mouse tibia after orchidectomy. J Bone Miner Res. 2008; 23:663–71. [PubMed: 18433300]
19. Lynch ME, Main RP, Xu Q, Schmicker TL, Schaffler MB, Wright TM, van der Meulen MC. Tibial compression is anabolic in the adult mouse skeleton despite reduced responsiveness with aging. Bone. 2011; 49:439–46. [PubMed: 21642027]
20. Main RP, Lynch ME, van der Meulen MC. In vivo tibial stiffness is maintained by whole bone morphology and cross-sectional geometry in growing female mice. J Biomech. 2010; 43:2689–94. [PubMed: 20673665]

21. De Souza RL, Matsuura M, Eckstein F, Rawlinson SC, Lanyon LE, Pitsillides AA. Non-invasive axial loading of mouse tibiae increases cortical bone formation and modifies trabecular organization: a new model to study cortical and cancellous compartments in a single loaded element. Bone. 2005; 37:810–8. [PubMed: 16198164]
22. Berlin O, Samid D, Donthineni-Rao R, Akeson W, Amiel D, Woods VL Jr. Development of a novel spontaneous metastasis model of human osteosarcoma transplanted orthotopically into bone of athymic mice. Cancer Res. 1993; 53:4890–5. [PubMed: 8402677]
23. Fritz V, Louis-Plence P, Apparailly F, Noël D, Voide R, Pillon A, Nicolas JC, Müller R, Jorgensen C. Micro-CT combined with bioluminescence imaging: a dynamic approach to detect early tumor-bone interaction in a tumor osteolysis murine model. Bone. 2007; 40:1032–40. [PubMed: 17251073]
24. Park BK, Zhang H, Zeng Q, Dai J, Keller ET, Giordano T, Gu K, Shah V, Pei L, Zarbo RJ, McCauley L, Shi S, Chen S, Wang CY. NF-kappaB in breast cancer cells promotes osteolytic bone metastasis by inducing osteoclastogenesis via GM-CSF. Nat Med. 2007; 13:62–9. [PubMed: 17159986]
25. Lanyon LE. Functional strain as a determinant for bone remodeling. Calcif Tissue Int. 1984; 36(Suppl 1):S56–61. [PubMed: 6430523]
26. Fritton JC, Myers ER, Wright TM, van der Meulen MC. Loading induces site-specific increases in mineral content assessed by microcomputed tomography of the mouse tibia. Bone. 2005; 36:1030–8. [PubMed: 15878316]
27. Pathi SP, Kowalczewski C, Tadipatri R, Fischbach C. A novel 3-D mineralized tumor model to study breast cancer bone metastasis. PLoS One. 2010; 5:e8849. [PubMed: 20107512]
28. Fischbach C, Chen R, Matsumoto T, Schmelzle T, Brugge JS, Polverini PJ, Mooney DJ. Engineering tumors with 3D scaffolds. Nat Methods. 2007; 4:855–60. [PubMed: 17767164]
29. Pathi SP, Lin DD, Dorvee JR, Estroff LA, Fischbach C. Hydroxyapatite nanoparticle-containing scaffolds for the study of breast cancer bone metastasis. Biomaterials. 2011; 32:5112–22. [PubMed: 21507478]
30. Ballyns JJ, Bonassar LJ. Dynamic compressive loading of image-guided tissue engineered meniscal constructs. J Biomech. 2011; 44:509–16. [PubMed: 20888562]
31. Sittichockechaiwut A, Scutt AM, Ryan AJ, Bonewald LF, Reilly GC. Use of rapidly mineralising osteoblasts and short periods of mechanical loading to accelerate matrix maturation in 3D scaffolds. Bone. 2009; 44:822–9. [PubMed: 19442630]
32. Sanchez C, Gabay O, Salvat C, Henrotin YE, Berenbaum F. Mechanical loading highly increases IL-6 production and decreases OPG expression by osteoblasts. Osteoarthritis Cartilage. 2009; 17:473–81. [PubMed: 18974013]
33. Minn AJ, Kang Y, Serganova I, Gupta GP, Giri DD, Doubrovin M, Ponomarev V, Gerald WL, Blasberg R, Massagué J. Distinct organ-specific metastatic potential of individual breast cancer cells and primary tumors. J Clin Invest. 2005; 115:44–55. [PubMed: 15630443]
34. Mancino AT, Klimberg VS, Yamamoto M, Manolagas SC, Abe E. Breast cancer increases osteoclastogenesis by secreting M-CSF and upregulating RANKL in stromal cells. J Surg Res. 2001; 100:18–24. [PubMed: 11516200]
35. Thomas RJ, Guise TA, Yin JJ, Elliott J, Horwood NJ, Martin TJ, Gillespie MT. Breast cancer cells interact with osteoblasts to support osteoclast formation. Endocrinology. 1999; 140:4451–8. [PubMed: 10499498]
36. Barnes GL, Hebert KE, Kamal M, Javed A, Einhorn TA, Lian JB, Stein GS, Gerstenfeld LC. Fidelity of Runx2 activity in breast cancer cells is required for the generation of metastases-associated osteolytic disease. Cancer Res. 2004; 64:4506–13. [PubMed: 15231660]
37. Javed A, Barnes GL, Pratap J, Antkowiak T, Gerstenfeld LC, van Wijnen AJ, Stein JL, Lian JB, Stein GS. Impaired intranuclear trafficking of Runx2 (AML3/CBFA1) transcription factors in breast cancer cells inhibits osteolysis in vivo. Proc Natl Acad Sci U S A. 2005; 102:1454–9. [PubMed: 15665096]
38. Bu G, Lu W, Liu CC, Selander K, Yoneda T, Hall C, Keller ET, Li Y. Breast cancer-derived Dickkopf1 inhibits osteoblast differentiation and osteoprotegerin expression: implication for breast cancer osteolytic bone metastases. Int J Cancer. 2008; 123:1034–42. [PubMed: 18546262]

39. Schmittgen TD, Livak KJ. Analyzing real-time PCR data by the comparative C(T) method. Nat Protoc. 2008; 3:1101–8. [PubMed: 18546601]
40. Chomczynski P, Sacchi N. Single-step method of RNA isolation by acid guanidinium thiocyanate-phenol-chloroform extraction. Anal Biochem. 1987; 162:156–9. [PubMed: 2440339]
41. Arrington SA, Schoonmaker JE, Damron TA, Mann KA, Allen MJ. Temporal changes in bone mass and mechanical properties in a murine model of tumor osteolysis. Bone. 2006; 38:359–67. [PubMed: 16278105]
42. Clohisy DR, Palkert D, Ramnaraine ML, Pekurovsky I, Oursler MJ. Human breast cancer induces osteoclast activation and increases the number of osteoclasts at sites of tumor osteolysis. J Orthop Res. 1996; 14:396–402. [PubMed: 8676252]
43. Mantila Roosa SM, Liu Y, Turner CH. Gene expression patterns in bone following mechanical loading. J Bone Miner Res. 2011; 26:100–12. [PubMed: 20658561]
44. Turner CH, Owan I, Alvey T, Hulman J, Hock JM. Recruitment and proliferative responses of osteoblasts after mechanical loading in vivo determined using sustained-release bromodeoxyuridine. Bone. 1998; 22:463–9. [PubMed: 9600779]
45. Forwood MR, Owan I, Takano Y, Turner CH. Increased bone formation in rat tibiae after a single short period of dynamic loading in vivo. Am J Physiol. 1996 Mar.270:E419–23. [PubMed: 8638687]
46. Lynch ME, Main RP, Xu Q, Walsh DJ, Schaffler MB, Wright TM, van der Meulen MC. Cancellous bone adaptation to tibial compression is not sex dependent in growing mice. J Appl Physiol. 2010; 109:685–91. [PubMed: 20576844]
47. Weilbaecher KN, Guise TA, McCauley LK. Cancer to bone: a fatal attraction. Nat Rev Cancer. 2011; 11:411–25. [PubMed: 21593787]
48. Sugiyama T, Meakin LB, Galea GL, Jackson BF, Lanyon LE, Ebetino FH, Russell RG, Price JS. Risedronate does not reduce mechanical loading-related increases in cortical and trabecular bone mass in mice. Bone. 2011; 49:133–9. [PubMed: 21497678]
49. Klein-Nulend J, Veldhuijzen JP, van Strien ME, de Jong M, Burger EH. Inhibition of osteoclastic bone resorption by mechanical stimulation in vitro. Arthritis Rheum. 1990; 33:66–72. [PubMed: 2302269]
50. Kobayashi Y, Hashimoto F, Miyamoto H, Kanaoka K, Miyazaki-Kawashita Y, Nakashima T, Shibata M, Kobayashi K, Kato Y, Sakai H. Force-induced osteoclast apoptosis in vivo is accompanied by elevation in transforming growth factor beta and osteoprotegerin expression. J Bone Miner Res. 2000; 15:1924–34. [PubMed: 11028444]
51. Boerckel JD, Uhrig BA, Willett NJ, Huebsch N, Guldberg RE. Mechanical regulation of vascular growth and tissue regeneration in vivo. Proc Natl Acad Sci U S A. 2011; 108:E674–80. [PubMed: 21876139]
52. Barnes GL, Javed A, Waller SM, Kamal MH, Hebert KE, Hassan MQ, Bellahcene A, Van Wijnen AJ, Young MF, Lian JB, Stein GS, Gerstenfeld LC. Osteoblast-related transcription factors Runx2 (Cbfa1/AML3) and MSX2 mediate the expression of bone sialoprotein in human metastatic breast cancer cells. Cancer Res. 2003; 63:2631–7. [PubMed: 12750290]
53. Pratap J, Wixted JJ, Gaur T, Zaidi SK, Dobson J, Gokul KD, Hussain S, van Wijnen AJ, Stein JL, Stein GS, Lian JB. Runx2 transcriptional activation of Indian Hedgehog and a downstream bone metastatic pathway in breast cancer cells. Cancer Res. 2008; 68:7795–802. [PubMed: 18829534]
54. Mendoza-Villanueva D, Zeef L, Shore P. Metastatic breast cancer cells inhibit osteoblast differentiation through the Runx2/CBFbeta-dependent expression of the Wnt antagonist, sclerostin. Breast Cancer Res. 2011; 13:R106. [PubMed: 22032690]
55. Kuperwasser C, Dessain S, Bierbaum BE, Garnet D, Sperandio K, Gauvin GP, Naber SP, Weinberg RA, Rosenblatt M. A mouse model of human breast cancer metastasis to human bone. Cancer Res. 2005; 65:6130–8. [PubMed: 16024614]
56. Almeida M, Han L, Martin-Millan M, O'Brien CA, Manolagas SC. Oxidative stress antagonizes Wnt signaling in osteoblast precursors by diverting beta-catenin from T cell factor- to forkhead box O-mediated transcription. J Biol Chem. 2007; 282:27298–305. [PubMed: 17623658]
57. Romas E, Gillespie MT. Inflammation-induced bone loss: can it be prevented? Rheum Dis Clin North Am. 2006; 32:759–73. [PubMed: 17288976]

58. Balkwill F, Mantovani A. Inflammation and cancer: back to Virchow? Lancet. 2001; 357:539–45. [PubMed: 11229684]

59. Frost HM. The regional acceleratory phenomenon: a review. Henry Ford Hosp Med J. 1983; 31:3–9. [PubMed: 6345475]

60. Zheng Y, Zhou H, Brennan K, Blair JM, Modzelewski JR, Seibel MJ, Dunstan CR. Inhibition of bone resorption, rather than direct cytotoxicity, mediates the anti-tumour actions of ibandronate and osteoprotegerin in a murine model of breast cancer bone metastasis. Bone. 2007; 40:471–8. [PubMed: 17092788]

61. Schwartz AL, Mori M, Gao R, Nail LM, King ME. Exercise reduces daily fatigue in women with breast cancer receiving chemotherapy. Med Sci Sports Exerc. 2001; 33:718–23. [PubMed: 11323538]

62. Winters-Stone KM, Dobek J, Bennett JA, Nail LM, Leo MC, Schwartz A. The effect of resistance training on muscle strength and physical function in older, postmenopausal breast cancer survivors: a randomized controlled trial. J Cancer Surviv. 2012; 6:189–99. [PubMed: 22193780]

63. Vainionpää A, Korpelainen R, Leppäluoto J, Jämsä T. Effects of high-impact exercise on bone mineral density: a randomized controlled trial in premenopausal women. Osteoporos Int. 2005; 16:191–7. [PubMed: 15221206]

64. Ozcivici E, Luu YK, Rubin CT, Judex S. Low-level vibrations retain bone marrow's osteogenic potential and augment recovery of trabecular bone during reambulation. PLoS One. 2010; 5:e11178. [PubMed: 20567514]

65. Parkinson DR, Dracopoli N, Petty BG, Compton C, Cristofanilli M, Deisseroth A, Hayes DF, Kapke G, Kumar P, Lee J, Liu MC, McCormack R, Mikulski S, Nagahara L, Pantel K, Pearson-White S, Punnoose EA, Roadcap LT, Schade AE, Scher HI, Sigman CC, Kelloff GJ. Considerations in the development of circulating tumor cell technology for clinical use. J Transl Med. 2012; 10:138. [PubMed: 22747748]

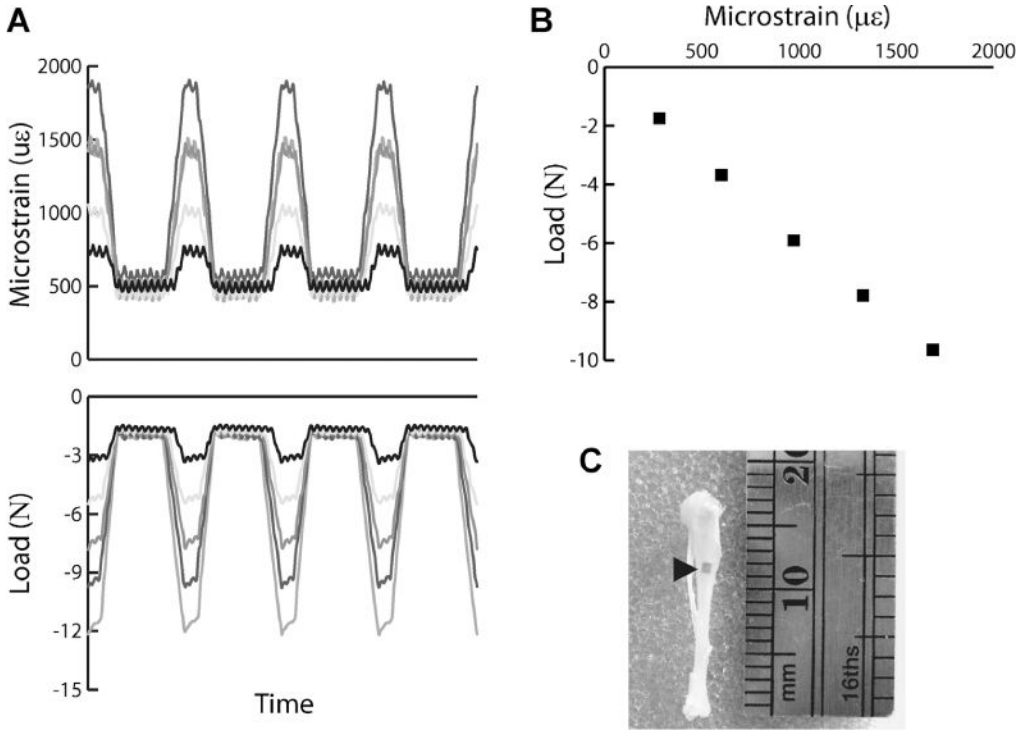


**Fig. 1.**

(*A*) Representative microstrain (με) and load (N) measurements recorded from a single-element strain gauge attached to the tibiae and an in-line load cell, respectively, during 1 second of tibial compression. (*B*) The strain-load relationship was determined from a linear regression relating the peak engendered strain and corresponding peak load during each load cycle.[20] From this relationship, we determined the 4.1 N applied peak force required to engender +600 με at the medial diaphysis of the tibia. (*C*) Image of a representative tibia with a strain attached to the medial diaphysis.

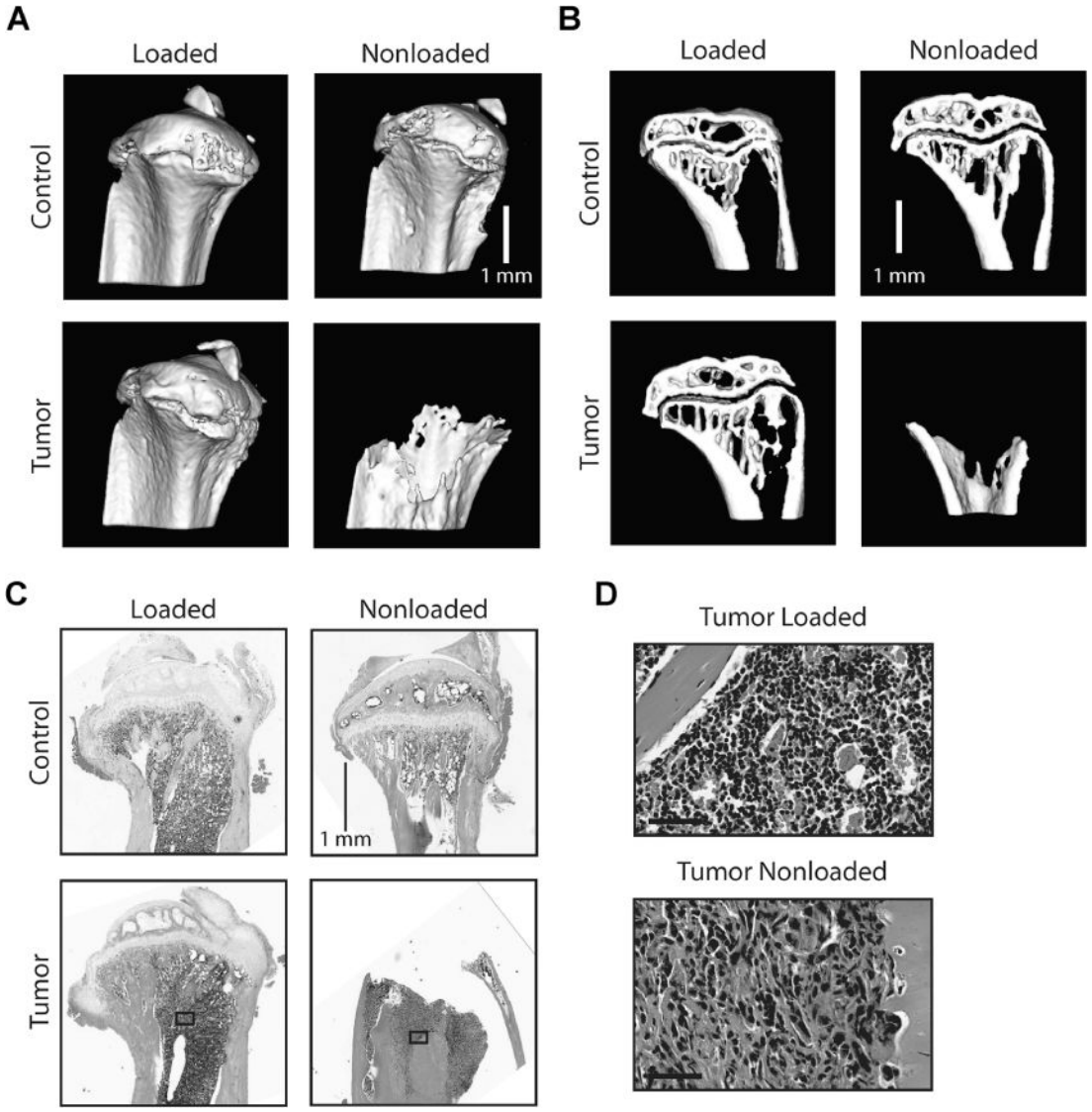


**Fig. 2.**

(*A*) 3D μCT reconstructions and (*B*) sagittal μCT sections of sham-injected (Control) and tumor-injected (Tumor) tibiae after 6 weeks as well as (*C*) corresponding representative H&E-stained histological cross-sections revealed that nonloaded tumor-bearing tibiae exhibited osteolytic degradation in the proximal compartment and extensive tumor formation, whereas loading inhibited these adverse changes. (*D*) High-powered images of the medullary space shown in *C* primarily indicate marrow cells in the tumor-injected loaded group, whereas tumor cells are abundant in the tumor-injected nonloaded group (bottom) (Bar = 50 μm). Representative images are shown. See Supplementary Figure 3 for color images.

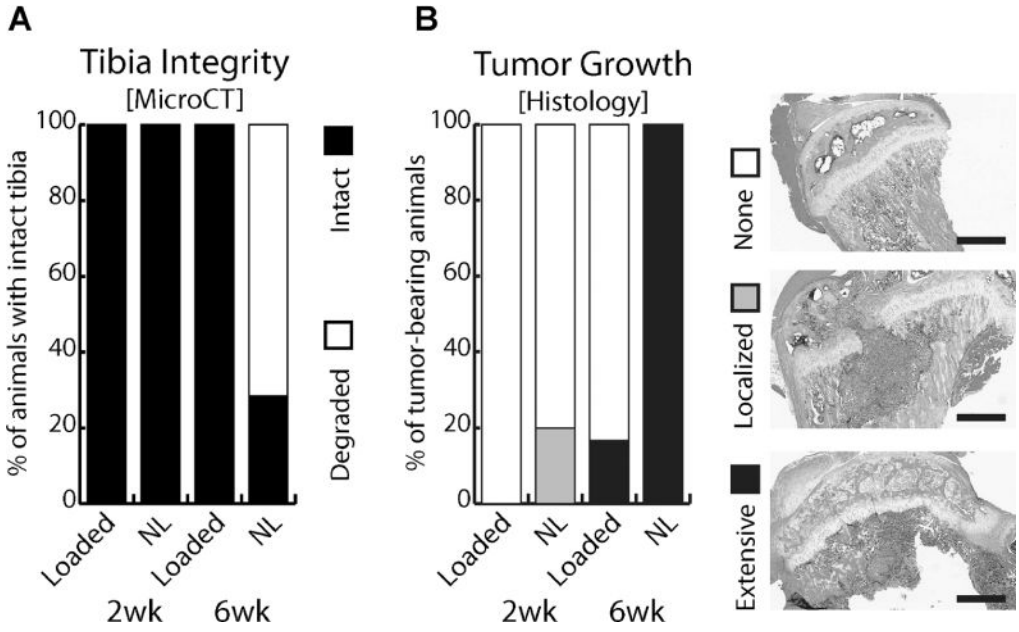


**Fig. 3.**

(*A*) Classification of tibiae for structural integrity. After 6 weeks, nearly all non-loaded (NL) tumor-bearing tibiae (71%) were extensively degraded, precluding μCT and statistical analysis, whereas no obvious changes were detected for loaded tumor-bearing tibiae. (*B*) Histological scoring of tibiae for tumor growth: None, Localized to injection site, or Extensive throughout the proximal metaphysis. Representative H&E-stained histological cross-sections are shown as the basis used for scoring. Bar = 500 μm. After 2 weeks, cancer cells remained localized to the injection site in 20% of nonloaded, tumor-injected tibiae, whereas after 6 weeks, all animals exhibited invasive tumor growth. Tibial compression significantly reduced these changes. See Supplementary Figure 4 for color images.

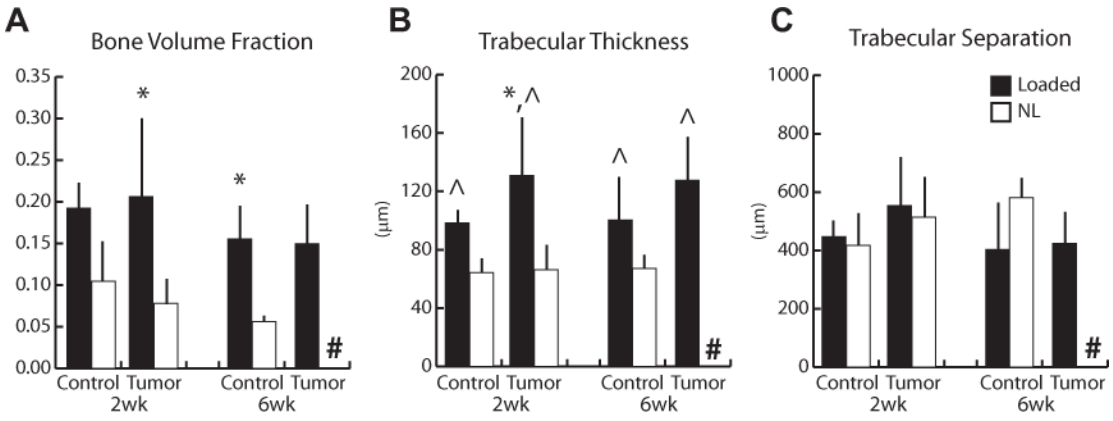


**Fig. 4.**

Indices of cancellous mass and architecture in sham-injected (Control) and tumor-injected (Tumor) animals via μCT. (*A*) After 2 weeks, bone volume fraction increased 160% with loading in the tumor-injected group; a similar, but not statistically significant, trend was noted in the sham-injected control group ($p = 0.1$). Bone volume fraction also increased 180% in the control group after 6 weeks (6-week tumor-injected group not analyzed). (*B*) Trabecular thickness increased 72% overall with loading (pooled Loaded versus pooled Control). (*C*) No differences in trabecular separation were observed among any groups, at any time point. #entire group excluded from analysis due to extensive degradation, *$p < 0.05$ versus corresponding nonloaded limbs, ^main effect of loading, $p < 0.05$ by linear mixed-model with repeated measures.

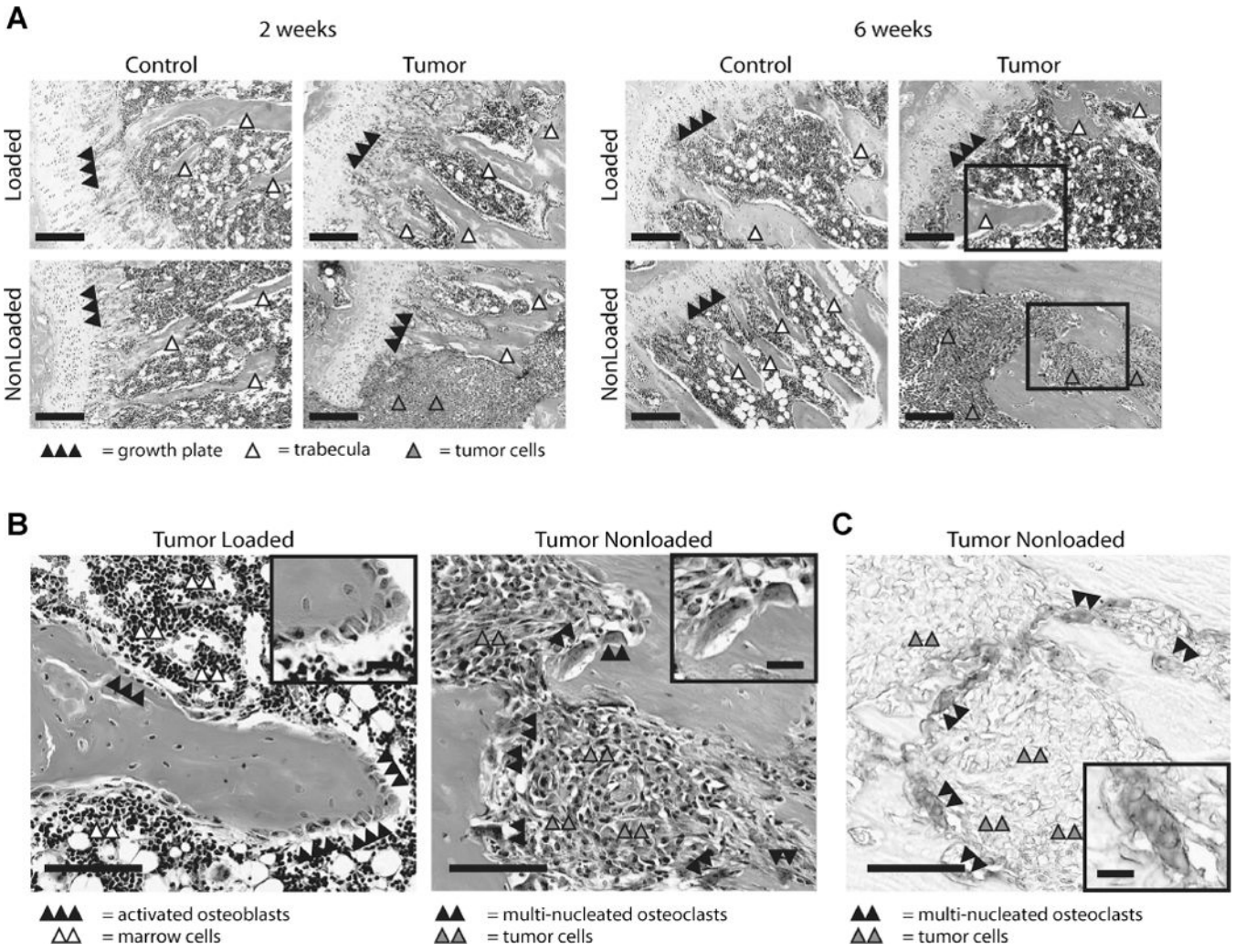


**Fig. 5.**

(*A*) Representative histological sections. Analysis of H&E stained sections indicated that tumor formation only occurred in 1 of 5 nonloaded tibiae after 2 weeks (shown) and was localized to the injection site. After 6 weeks, all nonloaded tumor-injected tibiae displayed evidence of tumor establishment and 6 of 7 tibiae showed extensive osteolysis. Only 1 of 7 loaded tumor-injected tibiae showed any evidence of tumor. Bar = 200 μm. (*B*) Images of representative cross sections from tumors in loaded and nonloaded tumors after 6 weeks (insets from *A*). Activated osteoblasts (inset bar = 25 μm) covered skeletal surfaces in loaded tibiae, whereas presence of multinucleated osteoclasts (inset bar = 25 μm) indicated bone degradation in nonloaded animals. Bar = 100 μm. (*C*) The presence of osteoclasts was further confirmed via subsequent TRAP staining of adjacent sections (inset bar = 25 μm). Bar = 100 μm. Supplementary Figure 5 for color images.

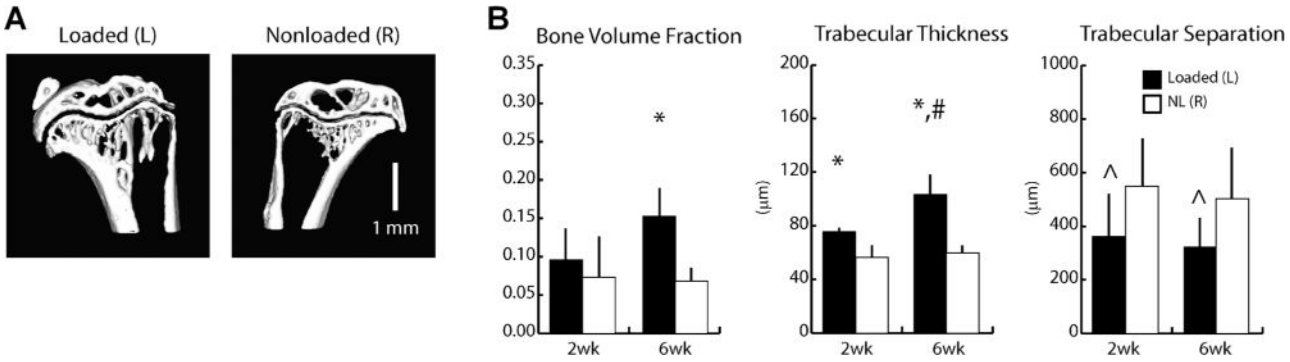


**Fig. 6.**

(*A*) Representative μCT images of loaded (left, L) and nonloaded (right, R) tibiae of intact SCID mice after 6 weeks of tibial compression. (*B*) Indices of cancellous mass and architecture via μCT. Bone volume fraction increased 130% after 6 weeks of loading. Trabecular thickness increased 34% after 2 weeks of loading, and 73% after 6 weeks. Trabecular separation decreased 35% with loading overall (pooled loaded versus pooled nonloaded). *Versus corresponding nonloaded limbs, #versus 2 week loaded limbs, ^main effect of loading, $p < 0.05$ by linear mixed-model with repeated measures.

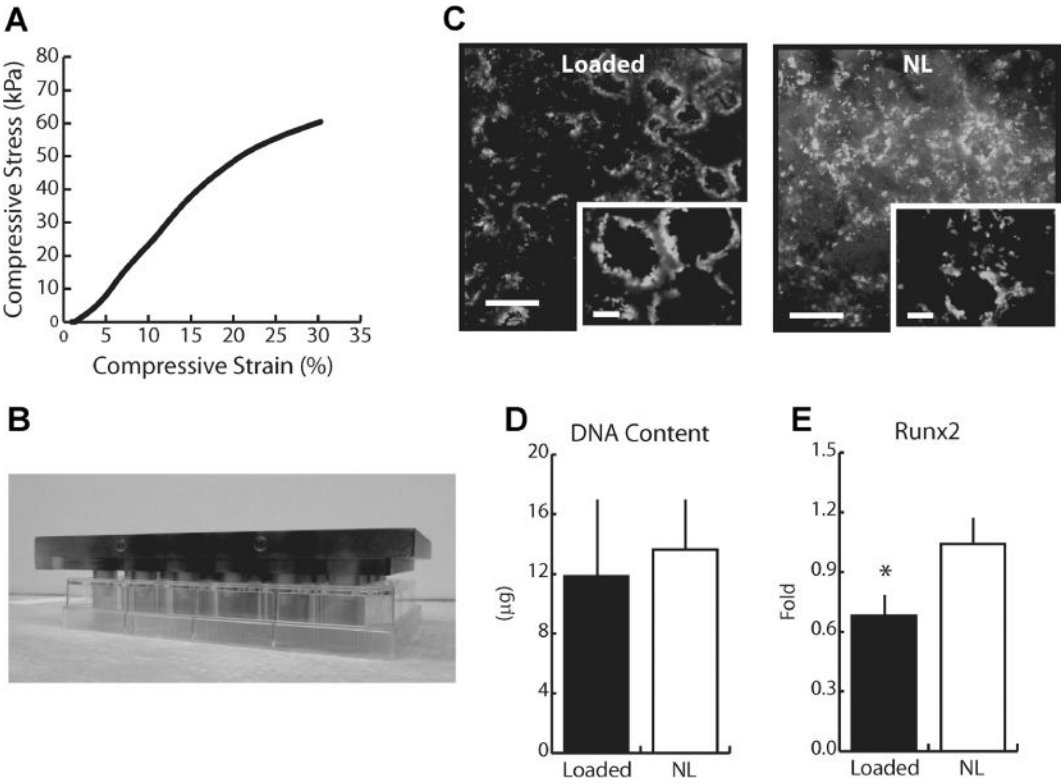


**Fig. 7.**

(*A*) Representative stress-strain curve for HA scaffolds undergoing quasi-static mechanical compression. The compressive yield strain and Young's modulus of the scaffolds were 290 ± 20 kPa and 29% ± 9% strain, respectively, ensuring that loading was performed within the linear elastic region of the HA scaffolds. (*B*) Loading platen utilized for loading tumor cell-seeded scaffolds in a 24-well culture plate for use in an established loading bioreactor.[30] (*C*) Representative image of live and dead staining with calcein (green) and propidium iodide (red). MDAs within scaffolds were not adversely affected by compressive loading. Bar = 500 µm (inset = 100 µm). (*D*) DNA content per scaffold as measured via fluorimetric analysis and (*E*) relative gene expression of Runx2 as determined via qPCR following 3 days of loading. DNA content was similar between MDAs in both loaded and culture scaffolds, whereas Runx2 expression was reduced 35% in loaded cultures. See Supplementary Figure 6 for color images.